Identification of Propagation Regimes on Integrated Microstrip Transmission Lines

Jonathan S. Bagby, Ching-Her Lee, Dennis P. Nyquist, and Yi Yuan

Abstract— **There has been a resurgence of interest in the propagation characteristics of open integrated microstrip transmission lines. This is due in part to the discovery of diverse propagation regimes for higher-order modes on open lines. In contrast to the dominant EH_0 mode, three distinct propagation regimes exist for higher-order modes on microstrip transmission lines. In this paper, a rigorous spectral-domain integral equation formulation is used to analyze propagation in all three regimes. This formulation provides a clear physical picture of the different propagation regimes based on the mathematical location of poles and branch points in the complex spectral-variable plane. As an illustration, the formulation is applied to the case of an isolated uniform microstrip transmission line. The integral equation is discretized via the method of moments, and entire-domain basis functions incorporating suitable edge behavior are utilized to provide convergence with relatively few terms. The results obtained are compared to the results of other workers, and good agreement is observed.**

I. Introduction

THERE has recently been a resurgence of interest in the propagation characteristics of open integrated microstrip transmission lines. This is primarily due to the discovery of diverse propagation regimes for higher-order modes on these lines. One such mode was described by Ermert [1] for closed microstrip structures, but its seeming nonphysical nature prompted him to reject these modes in his analysis. Later, Oliner [2], Grimm and Bagby [3], King [4], and Michalski and Zheng [5] described, in different fashions, three distinct propagation regimes for higher-order modes on microstrip transmission lines.

The first propagation regime, denoted here as the bound regime, is characterized by propagation constants that are real (in the low loss limit) and fields that are confined to the vicinity of the transmission line. The dominant EH_0 mode of an isolated microstrip line is an example of a mode in this regime (see [6] for a discussion of the dominant modes of identical coupled lines). The second propagation regime, the surface wave regime, is characterized by complex propagation constants with small imaginary parts, resulting in attenuation of the signal traversing the line (even when materials are assumed lossless). This attenuation is due to surface waves that are excited in the film layer of the integrated circuit background structure. The surface waves travel away from the axis of the transmission line, and energy from the transmission line mode is transferred to these unguided modes. The third propagation regime, the radiation regime, is characterized by complex propagation constants with large imaginary parts. In this case, losses occur from excitation of both surface waves in the film layer and radiation into the cover medium surrounding the open microstrip line. The existence of such leakage phenomena has been empirically verified for microstrip lines [7], and also for the related case of integrated dielectric waveguides [8].

In this paper, a powerful and rigorous spectral-domain integral equation formulation [9] is used to analyze propagation in all three regimes for integrated microstrip transmission lines. This formulation has the advantage of providing a clear physical picture of the different propagation regimes based on the mathematical location of poles and branch points in the complex spectral-variable plane. As an application, the formulation is applied to the case of an isolated open uniform integrated microstrip transmission line in a lossless surround. The integral equation is discretized via the method of moments, where entire-domain basis functions incorporating suitable edge behavior are utilized to permit closed-form evaluation of spatial integrals; convergence is attained with relatively few terms. The numerical results obtained in all three propagation regimes are compared to those of Oliner [2] and Michalski and Zheng [5], and good agreement is observed.

In Section II, the spectral-domain integral equation formulation is introduced. Based on the definition of mathematical parameters in the formulation, the three propagation regimes are identified and discussed in Section III. Section IV details the application of the method of moments to the integral equation. Numerical results are presented in Section V for the case of an isolated microstrip transmission line; dispersion curves and current distributions in all three propagation regimes are presented and compared to those obtained by others. A discussion of further applicability of these techniques

Manuscript received July 11, 1989; revised November 19, 1992. This work was supported by the Office of Navel Research under Contracts N00012-86-K-0424 and N00014-86-K-0609.

J. S. Bagby is with the Department of Electrical Engineering, Florida Atlantic University, Boca Raton, FL 33431.

C.-H. Lee is with the Department of Industrial Education, National Changhua University, Changhua, Taiwan 50058 R.O.C.

D. P. Nyquist is with the Department of Electrical Engineering, Michigan State University, East Lansing, MI 48824.

Y. Yuan is with the Department of Electrical Engineering, Michigan State University, East Lansing, MI. He is now with the Research Laboratory of Electronics, Department of Electrical Engineering and Computer Science, Massachusetts Institute of Technology, Cambridge, MA.

IEEE Log Number 9209333.

0018–9480/93$03.00 © 1993 IEEE

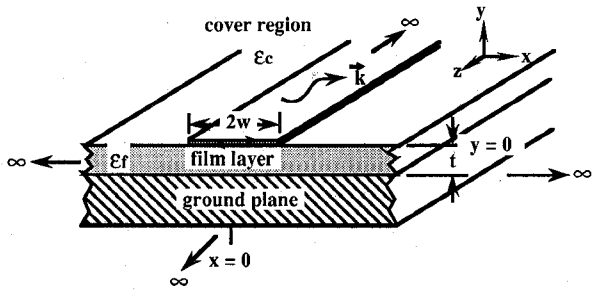

Fig. 1. Open microstrip transmission line of infinitesimal thickness on an infinite ground plane.

in analysis of microstrip transmission line and integrated dielectric waveguide systems is provided in Section VI.

II. Formulation

Consider the uniform open integrated microstrip transmission line geometry depicted in Fig. 1. The integral equation satisfied by the unknown natural-mode surface current $\vec{k}(\vec{\rho})$ on the line with an assumed propagation dependence of $\exp[j(\omega t - \zeta z)]$ is shown in [9] to be

$$\hat{t}\cdot\left(k_c^2+\tilde{\nabla}\tilde{\nabla}\cdot\right)\int_l \overleftrightarrow{g}(\vec{\rho}\,|\vec{\rho}\,';\zeta)\cdot\vec{k}(\vec{\rho}\,')\,dl' = 0; \qquad \vec{\rho}\in l\,. \tag{1}$$

Here, $\zeta = \beta - j\alpha$ is the unknown complex axial propagation constant of the natural mode, $\vec{k}(\vec{\rho})$ is the unknown natural-mode surface current, $\hat{t}$ is a unit tangent to the microstrip line, and $\tilde{\nabla}$ is the axially transformed del-operator, $\tilde{\nabla} = \nabla_t + j\zeta\hat{z}$. The electric Hertzian potential Green's dyad decomposes into a principal part and a reflected part, $\overleftrightarrow{g} = \overleftrightarrow{I}g^p + \overleftrightarrow{g}^r$, where $\overleftrightarrow{I}$ is the unit dyad, g^p is the two-dimensional unbounded space Green's function in integral form, and the reflected Green's dyad $\overleftrightarrow{g}^r$ has dyadic components

$$\overleftrightarrow{g}\,g^r = \hat{x}g_t\hat{x} + \hat{y}\left(\frac{\partial}{\partial x}g_c\hat{x} + g_n\hat{y} + j\zeta g_c\hat{z}\right) + \hat{z}g_t\hat{z}\,. \tag{2}$$

The scalar components of the reflected Green's dyad are given in terms of inversion integrals on the spectral variable ξ corresponding to x

$$\left.\begin{matrix} g_t \\ g_n \\ g_c \end{matrix}\right\} = \int_{-\infty}^{\infty}\left\{\begin{matrix} R_t(\lambda) \\ R_n(\lambda) \\ C(\lambda)\end{matrix}\right\}\frac{e^{j\xi(x-x')}e^{-p_c(y+y')}}{4\pi p_c}\,d\xi\,. \tag{3}$$

Here, $\lambda^2 = \xi^2 + \zeta^2$, and the wavenumber parameters p_c and p_f are defined by $p_c^2 = \lambda^2 - k_c^2$ and $p_f^2 = \lambda^2 - k_f^2$, where k_c and k_f are the wavenumbers in the cover region and film layer, respectively. Convergence considerations restrict our definitions of p_c and p_f to $\mathrm{Re}\{p_c\} > 0, \mathrm{Re}\{p_f\} > 0$ (which is a restriction of our choice of branch cuts in evaluating the square roots of p_c^2 and p_f^2, as discussed below). The reflection and coupling coefficients $R_t(\lambda), R_n(\lambda)$, and $C(\lambda)$ in the integrands of the reflected Green's dyad components are given by

$$R_t(\lambda) = \frac{p_c - p_f\coth(p_f t)}{p_c + p_f\coth(p_f t)} \qquad R_n\frac{Kp_c - p_f\tanh(p_f t)}{Kp_c + p_f\tanh(p_f t)}$$

$$C(\lambda) = \frac{2(K-1)p_c}{[p_c + p_f\coth(p_f t)][Kp_c + p_f\tanh(p_f t)]}, \qquad K = \frac{\varepsilon_f}{\varepsilon_c} \tag{4}$$

where ε_c and ε_f are the permittivities of the cover and film regions, respectively.

III. Propagation Regimes

The integrands of the spectral representation of the Green's dyad components in (3) contain the multivalued parameters p_c and p_f, defined above in terms of their squares: $p_c^2 = \lambda^2 - k_c^2$ and $p_f^2 = \lambda^2 - k_f^2$. Evaluation of the spectral inversion integrals on ξ in (3) requires a choice of branch cuts in the complex ξ-plane; so far, we have only the restrictions $\mathrm{Re}\{p_c\} > 0, \mathrm{Re}\{p_f\} > 0$ due to convergence considerations. Close examination reveals that all of the integrands are even functions of p_f, so a branch cut for this parameter is not implicated. Thus, the effects of a branch cut for p_f in the complex ξ-plane need not be further considered.

The integrands of the reflected Green's dyad also contain the singular coefficients $R_t(\lambda)$, $R_n(\lambda)$, and $C(\lambda)$. It can be shown that $R_t(\lambda)$ has a simple pole singularity when $\lambda = \lambda_p$ is a surface-wave eigenvalue of an odd TE mode of the width-doubled symmetric slab background structure. Similarly, $R_n(\lambda)$ has a simple pole singularity when $\lambda = \lambda_p$ is a surface-wave eigenvalue of an even TM mode of the width-doubled symmetric slab, and $C(\lambda)$ has simple poles at both odd TE and even TM surface-wave eigenvalues [3]. Indeed, setting $p_c = \gamma$ and $p_f = j\kappa$, the denominators of $R_t(\lambda)$, $R_n(\lambda)$, and $C(\lambda)$ have zeros when either $\cot\kappa = -\gamma/\kappa$ or $\tan\kappa t = \varepsilon_f\gamma/\varepsilon_c\kappa$. These are the familiar eigenvalue equations for even TE and odd TM modes of a symmetric slab waveguide of width $2t$.

To correctly locate the positions of the poles and branch points in the complex ξ-plane, it is first necessary to invoke material losses, and then consider the low-loss limiting case. Thus, we assume complex permittivities in the cover and film regions with $\varepsilon_c = \varepsilon_c' - j\varepsilon_c'', \varepsilon_f = \varepsilon_f' - j\varepsilon_f''$, where $\varepsilon_c'' > 0, \varepsilon_f'' > 0$. This implies that the wavenumber in the cover region, the surface-wave eigenvalues, and the microstrip propagation constant are also complex

$$k_c = k_{cr} - jk_{ci}; \qquad \lambda_p = \lambda_{pr} - j\lambda_{pi}; \qquad \zeta = \beta - j\alpha \tag{5}$$

where all real qualities above are assumed nonnegative.

Consider the surface wave eigenvalues λ_p. If λ_p is a surface wave eigenvalue of the background symmetric slab structure, corresponding poles of the Green's dyad integrand occur in the complex ξ-plane at values of ξ_p of ξ which give $\xi_p^2 + \zeta^2 = \lambda_p^2$. Substitution of (5) yields

$$\xi_p^2 = \lambda_p^2 - \zeta^2 = (\lambda_{pr}^2 - \lambda_{pi}^2 - \beta^2 + \alpha^2) - 2j(\lambda_{pr}\lambda_{pi} - \beta\alpha)\,. \tag{6}$$

We assume for convenience that the integrated circuit background structure supports only one surface wave, the dominant TM_0 slab waveguide mode, in frequency range of interest (which allows us to treat only a single pair of poles in the

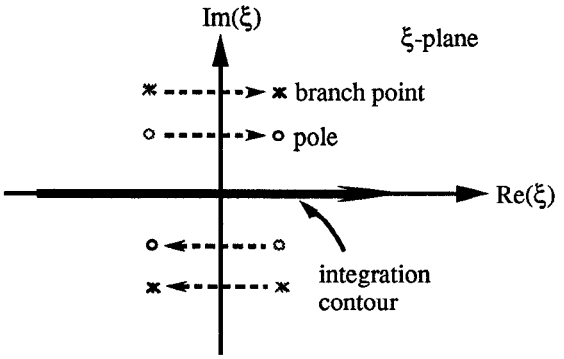

Fig. 2. Spectral integration contour and migration paths of poles and branch points in the bound regime.

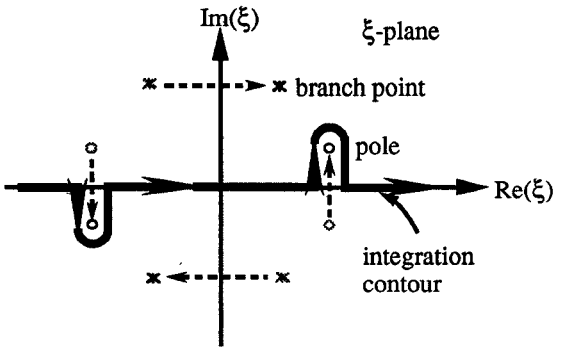

Fig. 3. Spectral integration contour and migration paths of poles and branch points for the surface wave regime (leaky regime 1 of Fig. 5).

complex ξ-plane). Treatment of more general case of multiple surface wave poles proceeds by extension of the analysis here.

Next consider the branch point ξ_b in the complex ξ-plane. The branch point ξ_b corresponds to the multivalued wavenumber parameter p_c, and occurs where

$$p_c^2 = \xi_b^2 + \zeta^2 - k_c^2 = 0$$

or, using (5),

$$\xi_b^2 = (k_{cr}^2 - k_{ci}^2 - \beta^2 + \alpha^2) - 2j(k_{cr}k_{ci} - \beta\alpha)\,. \quad (7)$$

Equations (6) and (7) will be used to identify the various propagation regimes based on the locations of ξ_p and ξ_b in the complex ξ-plane. This identification is based on a determination of the location of the poles and branch points with respect to the spectral inversion contour in the complex ξ-plane (i.e., the real ξ-axis). Depending on the locations of these singularities, inclusion of residues at poles or deformation around branch cuts may prove necessary. The characterization of different propagation regimes is accomplished by these considerations.

A. Bound Regime

We first treat the case where the transmission line mode propagation constant $\zeta = \beta - j\alpha$ satisfies the inequality $\mathrm{Re}\{\zeta^2\} > \mathrm{Re}\{\lambda_p^2\} > \mathrm{Re}\{k_c^2\}$. Using (5), this means that $\beta^2 - \alpha^2 > \lambda_{pr}^2 - \lambda_{pi}^2 > k_{cr}^2 - k_{ci}^2$. It will be shown that, in this case, the locations of the pole and branch singularities in the complex ξ-plane relative to the spectral inversion contour correspond to a microstrip mode in the bound regime.

First assume that material losses dominate, so that $\lambda_{pr}\lambda_{pi} > \beta\alpha$. By (6), this locates the initial position of the poles ξ_p in the complex ξ-plane in quadrants II and IV, as shown in Fig. 2. Similarly, (7) locates the branch-points ξ_b in the complex ξ-plane in quadrants II and IV. Now specialize to the lossless case by taking the low-loss limit such that $\beta\alpha$ becomes greater than $\lambda_{pr}\lambda_{pi}$ and $k_{cr}k_{ci}$. By (6) and (7), this is seen to produce a migration of the location of the poles and branch points in the complex ξ-plane into quadrants I and III respectively, as shown in the figure.

In this case, the migration of the poles and branch points as material losses vary does not cause them to cross the spectral inversion contour (the real ξ-axis). Therefore, in the bound regime, characterized by $\mathrm{Re}\{\zeta^2\} > \mathrm{Re}\{\lambda_p^2\} > \mathrm{Re}\{k_c^2\}$ (or in the lossless case, by a microstrip propagation constant greater than any surface wave eigenvalue), evaluation of spectral integrals in the expressions for the Green's dyad components can be performed in a straightforward fashion, with no special consideration given to pole and branch-point singularities in the complex ξ-plane.

B. Surface Wave Regime

Next, consider the case where the transmission line propagation constant ζ satisfies the inequality $\mathrm{Re}\{\lambda_p^2\} > \mathrm{Re}\{\zeta^2\} > \mathrm{Re}\{k_c^2\}$ or, by (5), $\lambda_{pr}^2 - \lambda_{pi}^2 > \beta^2 - \alpha^2 > k_{cr}^2 - k_{ci}^2$. It will be shown that this corresponds to a transmission line mode in the surface wave propagation regime.

Again, assume that material losses dominate, so that $\lambda_{pr}\lambda_{pi} > \beta\alpha$, which locates the initial positions of the poles and branch points in the complex ξ-plane in quadrants II and IV, as before. Next, take the low-loss limit so that $\beta\alpha$ is greater than $\lambda_{pr}\lambda_{pi}$ and $k_{cr}k_{ci}$; this results in the complex ξ-plane picture of Fig. 3. In this case, the surface wave poles have migrated from quadrants II and IV into quadrants III and I across the inversion contour, although the branch points once again migrate to quadrants I and III. Since the physical situation has not been altered by decreasing losses, the inversion contour should remain on the same side of the surface wave pole after taking the low-loss limit, as discussed by Boukamp and Jansen in [10].

These considerations indicate the necessity of deforming the inversion contour around the surface wave poles as shown in Fig. 3. Mathematically, this results in the inclusion of residue terms in the evaluation of the spectral integrals, which were absent in the previous case. Thus, when $\mathrm{Re}\{\lambda_p^2\} > \mathrm{Re}\{\zeta^2\} > \mathrm{Re}\{k_c^2\}$ (or, in the lossless case, when the transmission line phase constant lies between a surface wave eigenvalue and the wavenumber in the cover medium), residue contributions to the spectral integrals comprising the Green's dyad components cause the transmission line propagation constant ζ to become complex, even if materials are considered lossless. This corresponds to the physical effect of surface waves that are excited in the integrated circuit background structure, resulting in a decay in the transmission line mode ($\alpha > 0$). The surface waves travel in the film layer at an angle of $\cos^{-1}\beta/\lambda_{pr}$ to the transmission line axis [3].

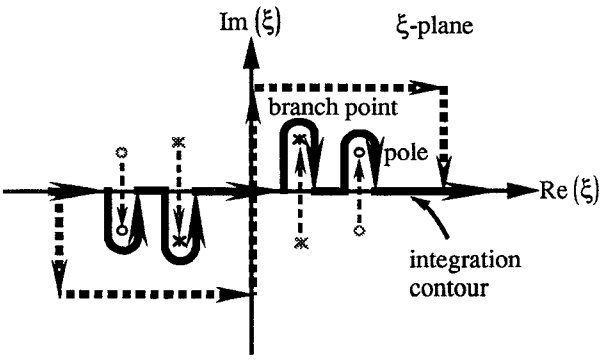

Fig. 4. Spectral integration contour and migration paths of poles and branch points for the radiation regime (leaky regime 2 of Fig. 5).

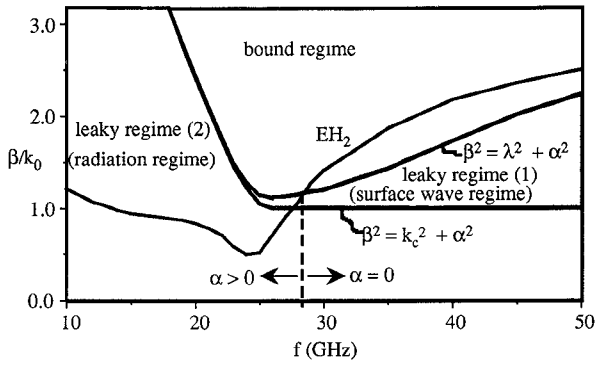

Fig. 5. Propagation regime diagram: the EH_2 mode is the second higher order mode of the microstrip shown in Fig. 1 with dimensions being strip width 3.0 mm, dielectric layer thickness 0.635 mm and $\varepsilon_r = 9.8$. In generating this figure the low loss limit has been assumed so that k_c and λ are purely real.

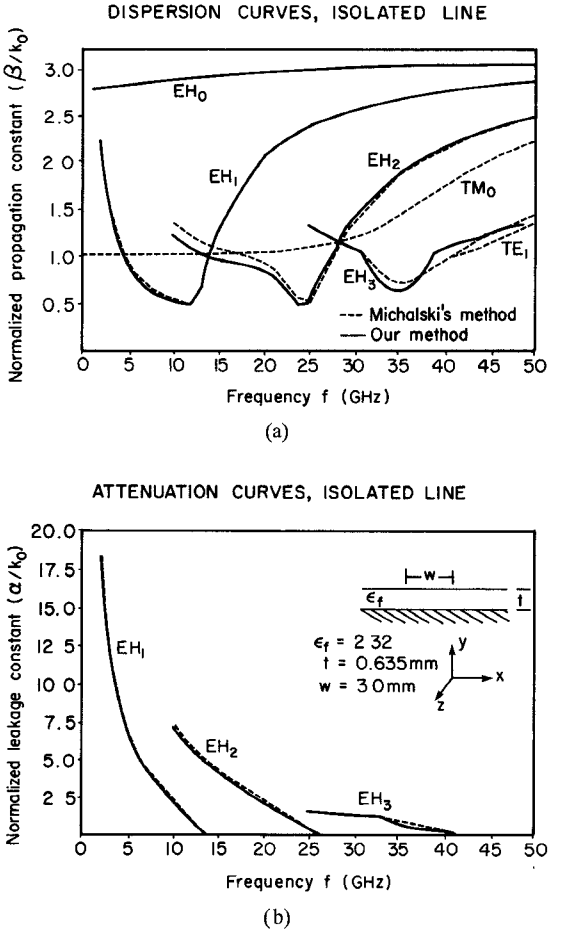

Fig. 6. Dispersion curves for the first three higher order modes of the microstrip structure shown in this figure: (a) phase constants; (b) attenuation constants.

C. Radiation Regime

The third propagation regime, the radiation regime, occurs when the microstrip propagation constant ζ satisfies the inequality $\mathrm{Re}\{k_c^2\} > \mathrm{Re}\{\zeta^2\}$ or, by (5), $k_{cr}^2 - k_{ci}^2 > \beta^2 - \alpha^2$. Again, allow material losses to dominate and then consider the low-loss case where $\beta\alpha$ is greater than $\lambda_{pr}\lambda_{pi}$ and $k_{cr}k_{ci}$. Equations (6) and (7) show that this results in both the poles and the branch points migrating from quadrants II and IV, across the contour of integration, into quadrants III and I, as depicted in Fig. 4. A similar effect is described in Assailly *et al.* [11]. As in the surface-wave regime case, this necessitates a deformation the contour of spectral integration around both the branch cuts and the surface wave poles as shown in the Figure. There is no unique way in which to deform the inversion contour, and different choices have been used by various workers [12].

The residue contributions at the surface wave poles again correspond physically to excitation of surface waves in the slab background structure. The contributions to the inversion integral along the portion of the contour which has been deformed around branch cuts correspond physically to the excitation of radiation in the open cover medium (specifically, radiation losses correspond to portions of the integration contour where $\arg(p_c) > \pi$). Propagation losses are quite large in the radiation regime, since radiation into the cover medium and excitation of surface waves in the film layer occur simultaneously. A dispersion diagram indicating the location of the three propagation regimes is provided in Fig. 5.

IV. MoM Solution

To apply (1) to the case of an isolated uniform microstrip transmission line, let the unit tangent and the microstrip current be decomposed as $\hat{t} = \hat{x}t_x + \hat{z}t_z$ and $\vec{k} = \hat{x}k_x + \hat{z}k_z$. Using a procedure similar to that in [13], k_x and k_z are expanded for a microstrip mode for even parity in terms of Chebyshev polynomials of the second and first kinds as follows:

$$k_x \cong \sqrt{1-\left(\frac{x'}{w}\right)^2}\sum_{n=0}^{N-1} a_n U_{2n+1}\left(\frac{x'}{w}\right),$$

$$k_z \cong \frac{1}{\sqrt{1-\left(\frac{x'}{w}\right)^2}}\sum_{n=0}^{N-1} b_n T_{2n}\left(\frac{x'}{w}\right). \tag{8}$$

Here, a_n and b_n are unknown expansion coefficients and the square-root factors in front of the summation terms yield the anticipated edge behavior. For the microstrip modes of odd parity, the same expansion are used with U_{2n+1} and T_{2n} replaced by U_{2n} and T_{2n+1}, respectively. Owing to even or odd symmetry of the currents, only even or odd orders of Chebshev polynomials are needed. The same functions are

used to test the equations in the longitudinal and transverse directions (Galerkin's method). The usual method of moments procedure results in appropriate equations for the open microstrip geometry. For the case of even parity, two coupled algebraic equations are obtained by letting $\hat{t}$ be $\hat{x}$ or $\hat{z}$:

$$\hat{x}: \sum_{n=0}^{N-1} a_n(-1)^n(n+1)\int_0^\infty \frac{k_c^2 R - \xi^2(R-C')}{p_c \xi^2} \cdot J_{2n+2}(w\xi)J_{2m+2}(w\xi)\,d\xi - j\sum_{n=0}^{N-1} b_n(-1)^n \frac{w}{2}\zeta \int_0^\infty \frac{R-C'}{p_c} \cdot J_{2n}(w\xi)J_{2m+2}(w\xi)\,d\xi = 0 \qquad M = 1,2,\cdots,N-1 \tag{9a}$$

$$\hat{z}: \sum_{n=0}^{N-1} a_n(-1)^n(n-1)\zeta \int_0^\infty \frac{R-C'}{p_c} \cdot J_{2n+2}(w\xi)J_{2m}(w\xi)\,d\xi - j\sum_{n=0}^{N-1} b_n(-1)^n \frac{w}{2}\int_0^\infty \cdot \frac{k_c^2 R - \zeta^2(R-C')}{p_c} J_{2n}(w\xi)J_{2m}(w\xi) \cdot d\xi = 0\,. \tag{9b}$$

Similar results hold in the case of odd parity.

This is a homogeneous system of $2N$ simultaneous algebraic equations for the $2N$ current expansion coefficients, and has nontrivial solution only for those values ζ_m of the propagation constant which render its determinant vanish. To obtain the propagation constants ζ_m of various modes, iterate (using Müller's method, for example) to search for the zeros of the determinant in the complex ζ-plane. In the bound regime, the zeros are real ($\alpha = o$) and belong to bound modes; however, in the leaky regimes (surface wave regime or radiation regime), the zeros are complex ($\zeta = \beta - j\alpha$) and correspond to leaky modes.

In numerical evaluation of the spectral inversion integrals, a path along the dashed line in Fig. 4 should be chosen whenever a surface wave pole near (or on) the real ξ-axis is encountered. In the radiation regime, while performing integration along the real ξ-axis in the interval $[0, \xi_b]$ (where radiation losses arise), the wavenumber parameter p_c, which involves a square root operation, must be negated if an intrinsic function (in a computer program) which takes the principal value of a square root is used. Due to the presence of the branch cut, the correct angle for p_c is 180° greater than its principal value.

Numerical results, including dispersion curves and current distributions, are provided in the next section and are compared to those of other techniques.

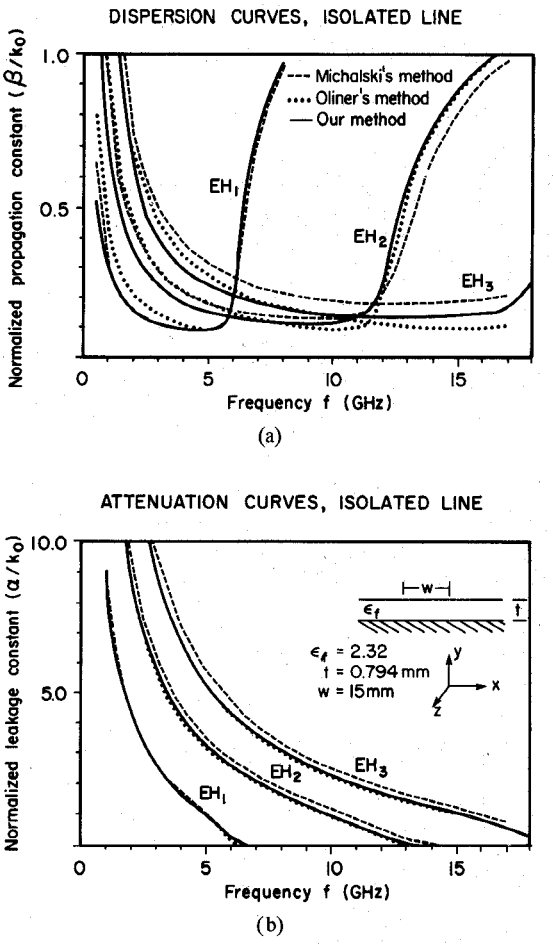

Fig. 7. Dispersion curves for the fundamental mode and the first three higher order modes of a microstrip geometry shown in this figure: (a) phase constants; (b) attenuation constants.

V. Numerical Results

Fig. 6 presents dispersion curves for the first three higher-order modes (EH_1, EH_2, and EH_3) for the open microstrip geometry of Fig. 1. This structure was previously analyzed by Oliner [2] using an asymptotic approach, and by Michalski and Zheng [5] utilizing a mixed-potential electric field integral equation. Results of all approaches are seen to agree well for EH_1 mode; the agreement is somewhat less favorable for higher-order modes.

Fig. 7 provides the dispersion characteristics of the fundamental and first three higher-order modes for a narrower microstrip line with a higher dielectric constant. This geometry was previously analyzed by Ermert [1] and Lee and Bagby [14] in the bound regime, and by Michalski and Zheng [5] in both the bound and leaky regimes. Results of the present analysis for the EH_0 and EH_1 modes agree well; the agreement is also quite good for the EH_2 mode. The dispersion curves labeled TM_0 and TE_1 in this figure represent the first two surface wave modes supported by the slab waveguide. When β/k_0 crosses the TM_0 curve, the corresponding microstrip mode enters the leaky regime.

Figs. 6 and 7 show that the leakage is large in lower frequency ranges, and loss due to leakage decreases as the

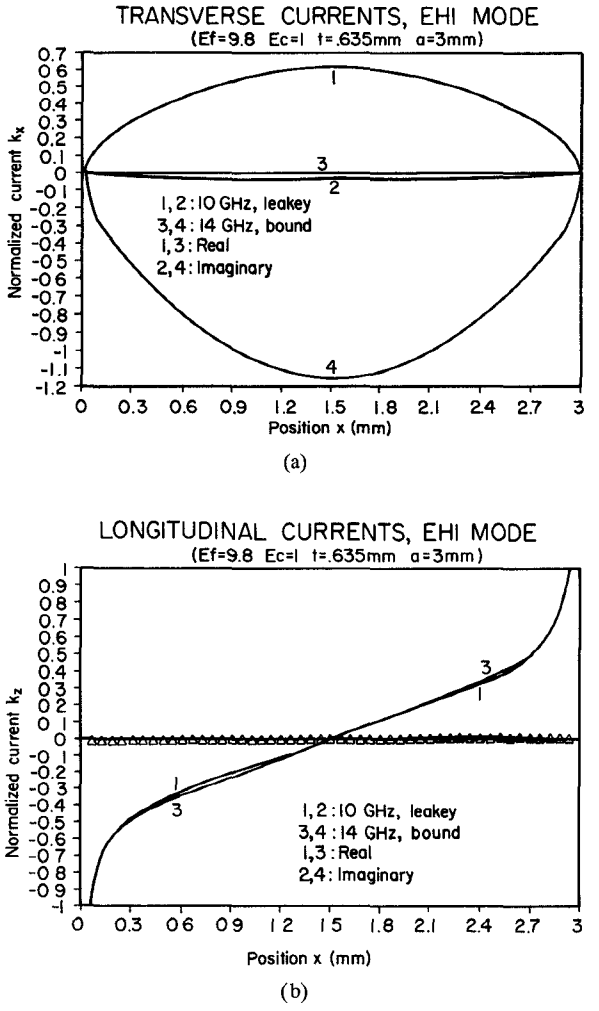

Fig. 8. (a) Transverse; and (b) longitudinal current distributions of the first higher order mode of the microstrip line depicted in Fig. 7.

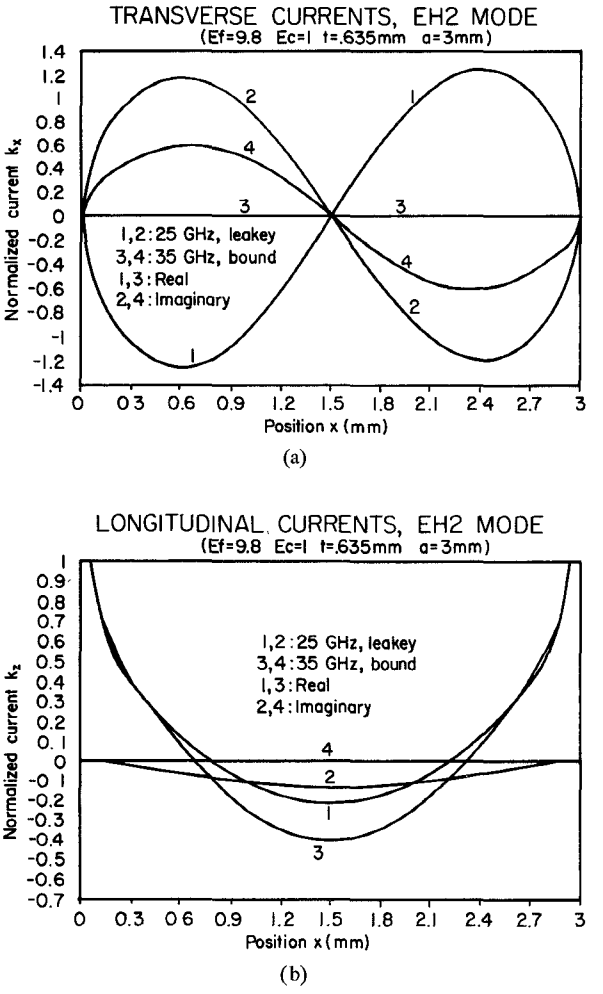

Fig. 9. (a) Transverse; and (b) longitudinal current distributions of the second higher order mode of the microstrip line shown in Fig. 7.

frequency increases, ultimately entering a bound regime where ζ is real ($\alpha = 0$).

Fig. 8, 9, and 10 present current distributions of the three higher-order modes of the narrow microstrip. The numbers 1, 3 and 4 represent the real and imaginary parts of currents corresponding to two different operating frequencies, respectively. Currents in each figure are normalized to have a maximum value of one. There is less change in the longitudinal current distribution than in the transverse current distribution as the microstrip mode passes from the bound regime to a leaky regime. Also, in the bound regime, the real part dominates the longitudinal current and the imaginary part dominates the transverse current, so the currents are 90° out of phase (as can be verified by the continuity equation [14]). However, this is not the case for leaky modes.

The same current distributions are obtained in Michalski and Zheng's work [5] using a subdomain basis method of moments technique. Comparison shows that the form of the currents are similar, whereas the magnitudes are different due differing normalization.

VI. Conclusions

In this paper, a spectral-domain integral equation formulation was used to analyze propagation in all three regimes for integrated microstrip transmission lines. This formulation provides a clear physical picture of the different propagation regimes based on the mathematical location of poles and branch points in the complex spectral-variable plane.

The formulation was applied to the case of an isolated uniform microstrip transmission line. Numerical results were obtained via the method of moments, where entire-domain basis functions incorporating the correct edge behavior were utilized to provide improved accuracy and convergence with relatively few terms. The results obtained compared favorably to those of other techniques.

Modification and extension of this work to the axial transform variable plane (the ζ-plane) is in progress, and further results are being obtained [15]. Other extensions of this effort include utilizing lossy modes in the design microstrip devices, and application of these concepts to the case of isolated and coupled integrated dielectric waveguides.

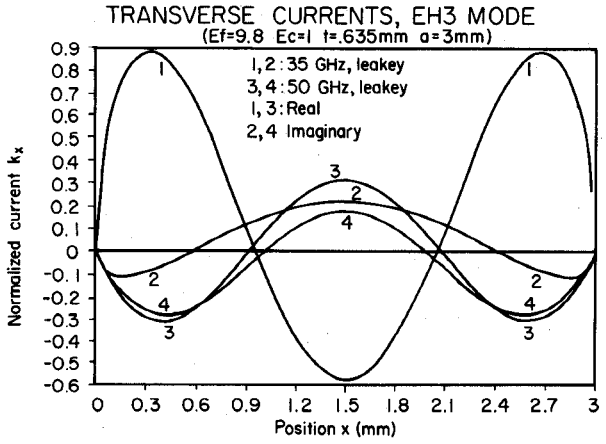

(a)

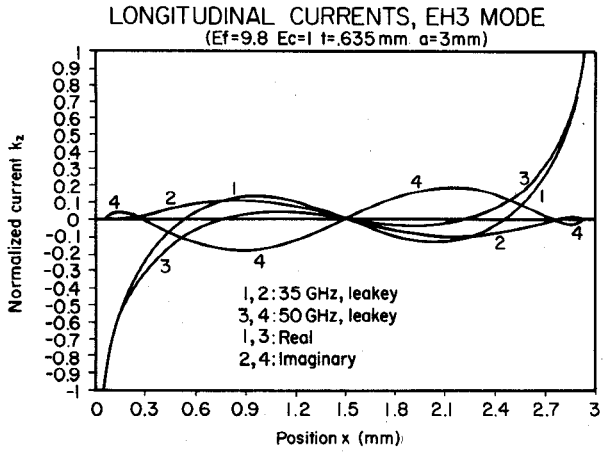

(b)

Fig. 10. (a) Transverse; and (b) longitudinal current distributions of the third higher order mode of the microstrip line shown in Fig. 7.

REFERENCES

[1] H. Ermert, "Guiding and radiation characteristics of planar waveguides," *IEEE Microwave, Opt., Acoust.*, vol. 3, pp. 59–62, Mar. 1979.

[2] A. A. Oliner, "Leakage from higher modes on microstrip line with application to antennas," *Radio Sci.*, vol. 22, no. 6, pp. 907–912, Nov. 1987.

[3] J. M. Grimm and J. S. Bagby, "Alternative integral formulation for analysis of microstrip transmission lines," in *Dig. Nat. Radio Sci. Meet.*, Boulder, CO, Jan. 1988, p. 113.

[4] R. P. W. King, "The propagation of signals along a three-layered region: Microstrip," *IEEE Trans. Microwave Theory Tech.*, vol. MTT-34, pp. 1080–1086, June 1988.

[5] K. A. Michalski and D. Zheng, "On the leaky modes of open microstrip lines," *Microwave Opt. Tech. Lett.*, vol. 2, no. 1, pp. 6–8, Jan. 1989.

[6] H. Shigesawa, M. Tsuji, and A. A. Oliner, "Dominant mode power leakage from printed-circuit waveguides," in *Proc. Int. Radio Sci. Symp.*, Stockholm, Sweden, Aug. 1989, pp. 527–529.

[7] R. German, E. F. Kuester, and D. C. Chang, "Experimental investigation of surface-wave radiation from a tapered dielectric slab," in *Dig. Nat. Radio Sci. Meet.*, Boulder, CO, Nov. 1989, p. 92.

[8] H. Shigesawa, M. Tauji, H. S. Myung, S. T. Peng, and A. A. Oliner, "Direct experimental confirmation of new leakage effects on open dielectric strip waveguides," in *Dig. Int. MTT Symp.*, 1983, pp. 293–295.

[9] J. S. Bagby and D. P. Nyquist, "Dyadic Green's functions for integrated electronic and optical circuits," *IEEE Trans. Microwave Theory Tech.*, vol. MTT-35, pp. 206–210, Feb. 1987.

[10] J. Boukamp and R. H. Jansen, "Spectral domain investigation of surface wave excitation and radiation by microstrip lines and microstrip disk resonators," in *Proc. Euro. Microwave Conf.*, Sept. 1983, pp. 721–726.

[11] S. Assailly, C. Terret, J. P. Daniel, G. Besnier, J. Mosig, and B. Roudot, "Spectral domain approach applied to open resonators: Application to microstrip antennas," *Electron. Lett.*, vol. 24, no. 2, pp. 105–106, Jan. 1988.

[12] K. A. Michalski and D. Zheng, "On the choice of branch cuts and integration paths in the analysis of open microstrip structures," *Electron. Lett.*, submitted.

[13] J. S. Bagby, C.-H. Lee, Y. Yuan, and D. P. Nyquist, "Entire-domain basis MOM analysis of coupled microstrip transmission lines," *IEEE Trans. Microwave Theory Tech.*, vol. MTT-40, Jan. 1992.

[14] C.-H. Lee and J. S. Bagby, "Analysis of coupled microstrip transmission lines with EFIE method," in *Dig. Int. IEEE-APS/URSI Symp.*, Syracuse, NY, June 1988, p. 318.

[15] D. P. Nyquist and J. M. Grimm, "Integral operator based spectral analysis for radiation modes of open-boundary waveguides," in *Dig. 14th Trienn. URSI Int. Symp. Electromag. Theory*, Sidney, Australia, Aug. 1992, p. 113.

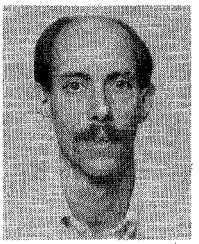

Jonathan S. Bagby was born in Denville, NJ, in 1957. He received the B.S. degree in 1980 from Michigan State University, the M.S. degree in 1981 from Ohio State University, and the Ph.D. degree from Michigan State University in 1984, all in electrical engineering.

From 1984 to 1991 he was an Assistant Professor of Electrical Engineering at the University of Texas at Arlington, and since 1991 he has been as Associate Professor of Electrical Engineering at Florida Atlantic University. His research interests include microwave integrated circuits, high-performance computing for electromagnetics, integrated optical circuits, electromagnetic radiation and scattering, and guided wave optics.

Dr. Bagby is a member of Eta Kappa Nu, Tau Beta Pi, Sigma Xi, and Phi Kappa Phi. He was the recipient of the 1983 MSU Excellence in Teaching Citation, and was named the UTA College of Engineering Outstanding Young Faculty Member in 1989.

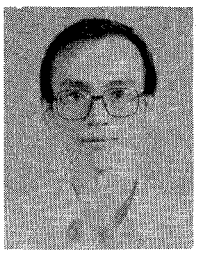

Ching-Her Lee was born in Pingtung, Taiwan, in 1954. He received the B.S. and M.S. degrees in electronic and automatic control engineering from Feng-Chia University in 1977 and 1981, respectively, and the Ph.D. degree in electrical engineering from the University of Texas at Arlington in 1989.

From 1981 to 1985 he was on the Faculty of Chin-Yih Institute of Technology, where he was the Head of the Electronic Engineering Department. While there, his specialty was high-frequency circuit design. He is currently as Associate Professor of National Changhau University of Education in Changhua, Taiwan. His research interests include microstrip devices, dielectric optical waveguides, and numerical methods in electromagnetics.

Dr. Lee is a member of Tau Beta Pi and the Chinese Institute of Engineers. He was the recipient of the Cash Award of Youth's Development and Invention and Award of Technical Invention in 1982, which is sponsored by the Ministry of Education, Republic of China.

Dennis P. Nyquist was born in Detroit, MI, in 1939. He received the B.S.E.E. and M.S.E.E. degrees in 1961 and 1964, respectively, and the Ph.D. degree in electrical engineering from Michigan State University, East Lansing, in 1966.

He joined the Faculty at MSU in 1966 and became Professor in 1979. His current research interests include electromagnetic interactions in integrated electronics, electromagnetic characterization of materials, and transient electromagnetics.

Dr. Nyquist is a member of Commission B of URSI, Sigma Xi, Tau Beta Pi, and Phi Kappa Phi. He was the recipient of the Michigan State University Teacher-Scholar Award in 1969.

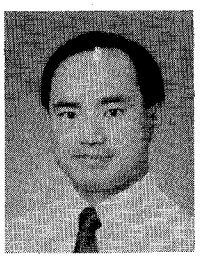

Yi Yuan was born in Jiangxi, China, in 1960. He received the B.S. degree in 1982 from Shandong University, the M.S. degree from Sichuan University, both in laser and electro-optics, and the Ph.D. degree in electrical engineering from Michigan State University in 1991.

From 1985 to 1987 he was on the Faculty of the Department of Physics, Sichuan University. From 1988 to 1991 he was a Graduate Research Assistant in the Department of Electrical Engineering at Michigan State University. Since 1991 he has been a Postdoctoral Research Associate in the Research Laboratory of Electronics, Department of Electrical Engineering and Computer Science, Massachusetts Institute of Technology. His present research interests include microwave integrated circuits, guided wave optics, and electromagnetic radiation and scattering.

Dr. Yuan is a member of Eta Kappa Nu, Sigma Xi, and Phi Beta Delta.